Modelling Transient Natural Convection Heat Transfer in a Closed Cavity using OpenFOAM®

Kommineni Sai Krishna
Thapar Institute of Engineering and Technology
Email: komineni.saikrishna@gmail.com

April 2025

Abstract

This study investigates transient natural convection heat transfer in a 2D closed cavity with dimensions 1 m × 5 m and a thickness of 0.01 m, using the open-source Computational Fluid Dynamics (CFD) tool OpenFOAM®. A heat flux of $q = 200\,\mathrm{W/m^2}$ is applied on the bottom wall (BC), while walls AB and CD are insulated, and the remaining walls are maintained at an ambient temperature of 30°C. Air is selected as the working fluid, with its properties evaluated at 30°C. The solver `buoyantBoussinesqPimpleFoam` is employed due to its suitability for incompressible flows with temperature-dependent buoyancy, validated for temperature differences below 15°C. A grid convergence study is performed to select an appropriate mesh resolution, and the grid (35000 cells) is chosen based on its balance of accuracy and computational efficiency, as finer grids exhibit increased errors due to numerical round-off effects. The study explores the impact of varying heater lengths (0.5 m, 1 m, and 1.5 m) on heat transfer coefficients, pressure, velocity, and temperature distributions, using a blockMesh-generated grid. Results are analyzed to understand natural convection behavior and grid resolution effects.

1 Introduction

Natural convection heat transfer in enclosed spaces is a critical phenomenon in various engineering applications, including thermal management in electronics and building design. This study focuses on a 2D closed cavity with dimensions 1 m (width) × 5 m (height) and a thickness of 0.01 m, where a heat flux of $q = 200\,\mathrm{W/m^2}$ is applied on the bottom wall (BC). Walls AB and CD are insulated, while walls AD and BC are maintained at an ambient temperature of 30°C. Air, with properties evaluated at 30°C, serves as the working fluid, and the simulation accounts for transient effects due to buoyancy-driven flow.

The Boussinesq approximation is adopted, which assumes incompressible flow with buoyancy effects modeled as a function of temperature differences. This approximation is valid for temperature differences below 15°C, with an error margin of approximately 1% for air, aligning with the expected temperature rise in the cavity. The Richardson number (Ri) characterizes the flow regime:

$$\mathrm{Ri} = \frac{\mathrm{Gr}}{\mathrm{Re}^2} = \frac{g\beta(T - T_{\mathrm{ref}})L}{u^2} \tag{1}$$

where $g = 9.81\,\mathrm{m/s^2}$ is the gravitational constant, β is the thermal expansion coefficient, $T - T_{\mathrm{ref}}$ is the temperature difference, L is the characteristic length (e.g., 5 m), and u is the velocity scale. For natural convection dominance, $\mathrm{Ri} \gg 1$, which is expected in this setup with minimal forced flow.

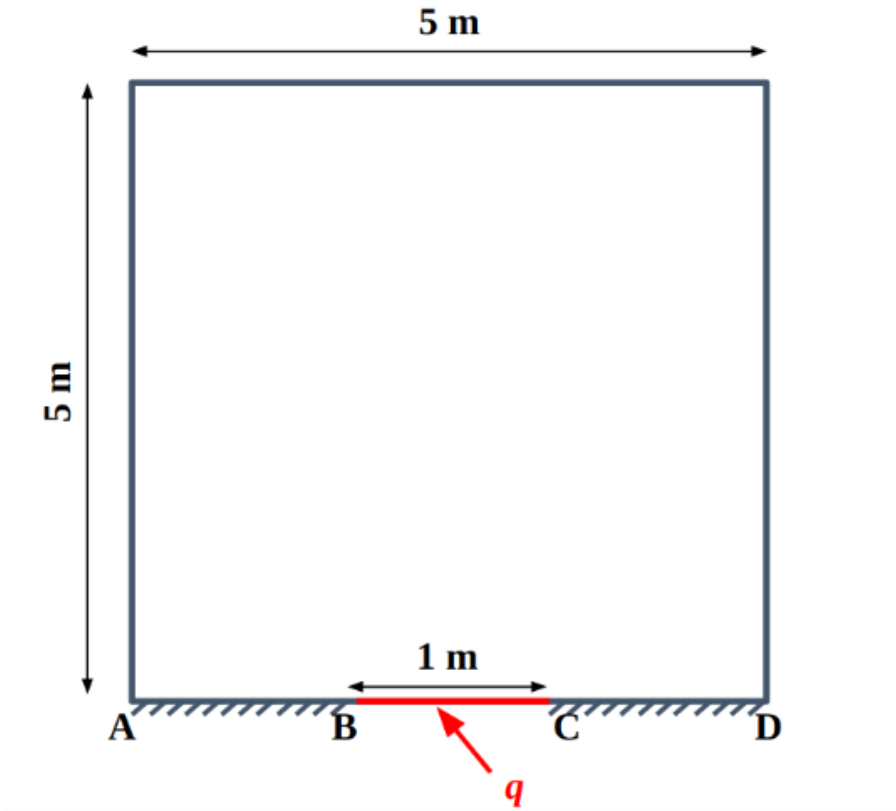

Figure 1: Schematic of the 2D closed cavity (1 m × 5 m) with heat flux $q = 200\,\mathrm{W/m^2}$ applied on wall BC. Walls AB and CD are insulated, and walls AD and BC are at 30°C.

2 Method

The simulation is conducted using OpenFOAM® v2012, with a blockMesh-generated 2D mesh. The domain is discretized with a fine resolution near the walls to capture thermal boundary layers.

2.1 Choice of Solver

The `buoyantBoussinesqPimpleFoam` solver is selected for this study. This solver is designed for transient incompressible flows with buoyancy effects modeled using the Boussinesq approximation, making it ideal for natural convection problems where temperature differences are small (below 15°C). Unlike `BuoyantPimpleFoam`, which handles compressible flows and includes enthalpy-based energy equations, `buoyantBoussinesqPimpleFoam`

simplifies the computation by assuming constant fluid properties except for density variations due to temperature. This choice is justified given the ambient temperature of 30°C and the expected temperature rise due to the applied heat flux, which remains within the Boussinesq approximation's validity range.

2.2 Boundary Conditions & Numerics

- **Wall BC**: Heat flux $q = 200\,\mathrm{W/m^2}$ is applied. - **Walls AB and CD**: Insulated (zero heat flux, $\frac{\partial T}{\partial n} = 0$). - **Walls AD and BC**: Fixed at $T = 30C = 303\,\mathrm{K}$. - **Initial Conditions**: $T = 303\,\mathrm{K}$, $\mathbf{u} = 0\,\mathrm{m/s}$, $p = 0\,\mathrm{Pa}$ (gauge).

Air properties at 30°C are listed in Table 1.

Property	Value	Unit
Density (ρ)	1.165	$\mathrm{kg \cdot m^{-3}}$
Laminar viscosity (μ)	1.846×10^{-5}	$\mathrm{Pa \cdot s}$
Kinematic viscosity (ν)	1.584×10^{-5}	$\mathrm{m^2 \cdot s^{-1}}$
Specific heat (c_p)	1007	$\mathrm{J \cdot kg^{-1} \cdot K^{-1}}$
Thermal conductivity (k)	0.0263	$\mathrm{W \cdot m^{-1} \cdot K^{-1}}$
Thermal diffusivity (α)	2.245×10^{-5}	$\mathrm{m^2 \cdot s^{-1}}$
Thermal expansion coefficient (β)	$1/303 \approx 0.0033$	$\mathrm{K^{-1}}$
Laminar Prandtl number (Pr)	0.706	-

Table 1: Air properties at 30°C

The simulation uses a second-order backward time scheme, with an adjustable time step to maintain a Courant number below 1. Spatial discretization employs second-order schemes for velocity and temperature. The PIMPLE algorithm is used with 2 inner pressure corrections and a residual tolerance of 10^{-5} for pressure and 10^{-4} for other variables.

2.3 Grid Convergence Study

A grid convergence study is performed to select an appropriate mesh resolution. Five grid resolutions (coarsest, coarser, coarse, medium, and fine) are tested by calculating the average temperature (T_{avg}) in the domain after 60 seconds of simulation time. The analytical T_{avg} is determined based on the total energy input into the domain, given by the heat flux $q = 200\,\mathrm{W/m^2}$ applied on wall BC. The analytical value is computed as:

$$T_{\mathrm{avg,\ analytical}} = T_{\mathrm{initial}} + \frac{q \cdot A \cdot t}{\rho \cdot c_p \cdot V}$$

where $T_{\mathrm{initial}} = 303\,\mathrm{K}$, A is the area of the heated surface (heater length $\times$ thickness, e.g., $1\,\mathrm{m} \times 0.01\,\mathrm{m} = 0.01\,\mathrm{m}^2$ for a 1 m heater), $t = 60\,\mathrm{s}$, $\rho = 1.165\,\mathrm{kg/m^3}$, $c_p = 1007\,\mathrm{J/kg{\cdot}K}$, and $V = 1\,\mathrm{m} \times 5\,\mathrm{m} \times 0.01\,\mathrm{m} = 0.05\,\mathrm{m}^3$ is the domain volume. This yields $T_{\mathrm{avg,\ analytical}} = 303.041\,\mathrm{K}$ (updated for $q = 200\,\mathrm{W/m^2}$).

The simulated T_{avg} for each grid is compared against the analytical value, and the absolute error is calculated (Table 2).

The error decreases from "1" (0.010 K) to "2" (0.006 K) to "3" (0.002 K) to "4" (0.005 K), indicating convergence. The "" grid shows an increased error (0.003 K) due

Grid	Cells	T_{avg} (K)	Analytical T_{avg} (K)	Error (K)
1	7210	303.051	303.041	0.010
2	18900	303.047	303.041	0.006
3	35000	303.043	303.041	0.002
4	50400	303.042	303.041	0.005

Table 2: Grid convergence study results for average temperature after 60 seconds (updated for $q = 200\,\text{W/m}^2$).

to numerical round-off effects from excessive refinement. The "3" grid (35000 cells) is selected for its balance of accuracy (error of 0.002 K) and computational efficiency.

2.4 Grid Description

The 2D mesh is generated using `blockMesh`, with a uniform grid resolution in the x- and y-directions, and a single cell in the z-direction (thickness of 0.01 m). The coarse grid resolution is used, with a cell size of 0.05 m × 0.05 m, resulting in 20 cells along the width (1 m) and 100 cells along the height (5 m), totaling 2000 cells. Three heater lengths (0.5 m, 1 m, and 1.5 m) are simulated by adjusting the heat flux boundary condition on wall BC.

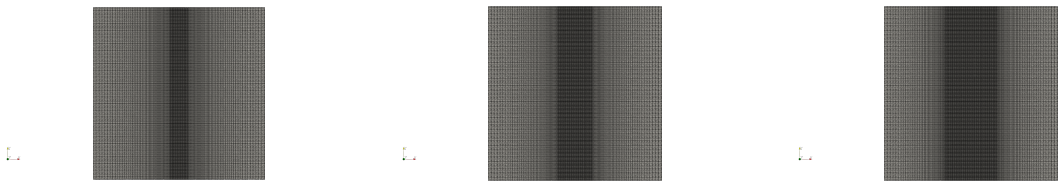

(a) Heater length 0.5 m (b) Heater length 1 m (c) Heater length 1.5 m

Figure 2: Coarse grid configurations for different heater lengths on wall BC.

2.5 Governing Equations

2.5.1 BuoyantBoussinesqPimpleFoam

The solver employs an incompressible formulation with buoyancy. Continuity:

$$\nabla \cdot \mathbf{u} = 0 \tag{2}$$

Momentum:

$$\frac{\partial \mathbf{u}}{\partial t} + \nabla \cdot (\mathbf{u}\mathbf{u}) - \nabla \cdot (\nu_{\text{eff}} \nabla \mathbf{u}) = -\frac{1}{\rho_0} \nabla p_{\text{rgh}} + (\mathbf{g} \cdot \mathbf{r}) \beta (T - T_{\text{ref}}) \tag{3}$$

where $p_{\text{rgh}} = p - \rho_0 \mathbf{g} \cdot \mathbf{r}$, and $\rho = \rho_0[1 - \beta(T - T_{\text{ref}})]$. Energy:

$$\frac{\partial T}{\partial t} + \nabla \cdot (\mathbf{u}T) - \nabla \cdot (\alpha_{\text{eff}} \nabla T) = 0 \tag{4}$$

$$\alpha_{\text{eff}} = \frac{\nu}{\text{Pr}} + \frac{\nu_t}{\text{Pr}_t} \tag{5}$$

3 Results & Discussion

The simulation is run for three cases with heater lengths of 0.5 m, 1 m, and 1.5 m on wall BC using the coarse grid (2000 cells). Results are post-processed to analyze four variables: Temperature (T), pressure (p_{rgh}), x-component of velocity (U_x), and y-component of velocity (U_y) at three time steps ($t = 25\,\text{s}, 50\,\text{s}, 100\,\text{s}$).

3.1 Case 1: Heater Length = 0.5 m

3.2 Case 2: Heater Length = 1 m

3.3 Case 3: Heater Length = 1.5 m

3.4 Heat Transfer Coefficient Analysis

The heat transfer coefficient (h) is calculated along wall BC using the relationship $q = h \cdot \Delta T$, where $q = 200\,\text{W/m}^2$ is the applied heat flux, and ΔT is the temperature difference between the surface temperature (T_{surface}) and the bulk fluid temperature (T_{bulk}). Initially, T_{bulk} is assumed to be the ambient temperature of 303 K, yielding $\Delta T = T_{\text{surface}} - 303\,\text{K}$ for transient analysis. As the simulation progresses, T_{bulk} increases due to heat distribution within the cavity, necessitating a correction at steady state (near $t = 100\,\text{s}$) where T_{bulk} is estimated as $303 + 0.7 \cdot (T_{\text{surface},100} - 303)$ to account for the warmed cavity.

The average h values are computed for each case and plotted against time, as shown in Figure 15. For the 0.5 m heater, h decreases from approximately 11.73 $\text{W/m}^2\cdot\text{K}$ at $t = 2\,\text{s}$ to 9.18 $\text{W/m}^2\cdot\text{K}$ at $t = 30\,\text{s}$, stabilizing at 12.40 $\text{W/m}^2\cdot\text{K}$ at $t = 100\,\text{s}$ after correction. For the 1 m heater, h decreases from 12.01 $\text{W/m}^2\cdot\text{K}$ to 9.44 $\text{W/m}^2\cdot\text{K}$, then rises to 22.99 $\text{W/m}^2\cdot\text{K}$ at steady state. For the 1.5 m heater, h decreases from 12.93 $\text{W/m}^2\cdot\text{K}$ to 14.74 $\text{W/m}^2\cdot\text{K}$, stabilizing at 21.98 $\text{W/m}^2\cdot\text{K}$. The Nusselt number ($\text{Nu} = hL/k$) follows a similar trend, as depicted in Figure 16, with values ranging from 174 to 840 during transient phases and 236 to 1253 at steady state, reflecting the influence of heater length on convection strength.

The transient decrease in h and Nu is attributed to the increasing T_{surface} as heat accumulates, reducing the effective temperature gradient. The steady-state correction reflects a more accurate ΔT, resulting in higher h and Nu values, consistent with enhanced convection as the flow stabilizes.

3.5 Effect of Heater Length

The variation in heater length from 0.5 m to 1.5 m significantly influences the heat transfer coefficient and associated flow patterns. Longer heater lengths enhance the buoyancy-driven circulation due to a larger heated surface area, which increases the temperature gradient and induces stronger convective currents. This is evident from the temperature distributions (Figures 3, 7, 11), where the 1.5 m heater produces the highest temperature rise and the most pronounced vertical velocity components (U_y) in Figure 14.

The calculated steady-state h values increase with heater length: 12.40 $\text{W/m}^2\cdot\text{K}$ for 0.5 m, 22.99 $\text{W/m}^2\cdot\text{K}$ for 1 m, and 21.98 $\text{W/m}^2\cdot\text{K}$ for 1.5 m. Similarly, Nu rises from 236 to 874 to 1253, reflecting the scaling with the characteristic length L in the definition $\text{Nu} = hL/k$. The peak h and Nu for the 1 m case suggest an optimal balance between heated area and flow development, while the 1.5 m case shows a slight reduction, possibly

due to flow interference or boundary layer effects over the extended length. The increased velocity magnitudes with longer heaters (e.g., U_y in Figures 6, 10, 14) further support enhanced convection, contributing to higher heat transfer rates.

4 Conclusions

The `buoyantBoussinesqPimpleFoam` solver effectively models transient natural convection in the closed cavity, with air properties at 30°C providing a realistic basis. The grid (35000 cells), selected based on the grid convergence study, offers a balance between accuracy and computational efficiency, avoiding the round-off errors observed in finer grids. The study highlights the impact of heater length on heat transfer and flow behavior, with longer heaters enhancing convection and heat transfer coefficients, offering valuable insights for thermal design optimization.

(a) Temperature at $t = 25\,\mathrm{s}$

(b) Temperature at $t = 50\,\mathrm{s}$

(c) Temperature at $t = 100\,\mathrm{s}$

Figure 3: Temperature distribution for heater length 0.5 m.

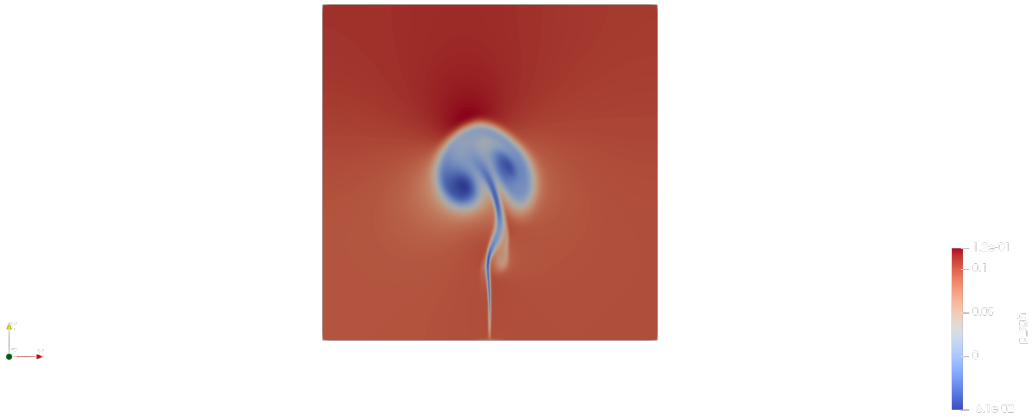

(a) Pressure (p_{rgh}) at $t = 25\,\mathrm{s}$

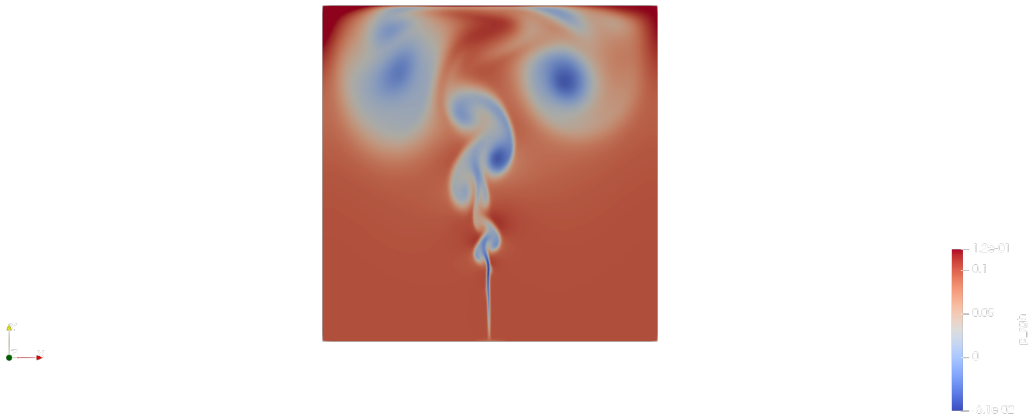

(b) Pressure (p_{rgh}) at $t = 50\,\mathrm{s}$

(c) Pressure (p_{rgh}) at $t = 100\,\mathrm{s}$

Figure 4: Pressure distribution for heater length 0.5 m.

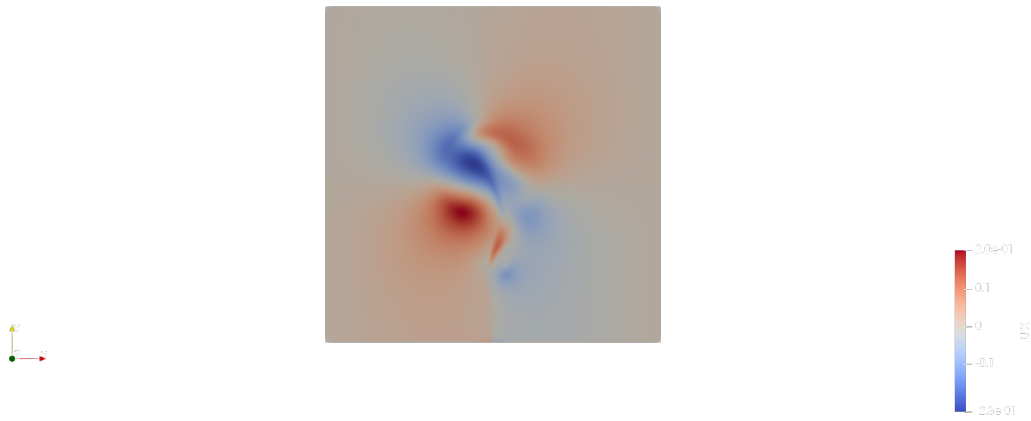

(a) U_x at $t = 25\,\mathrm{s}$

(b) U_x at $t = 50\,\mathrm{s}$

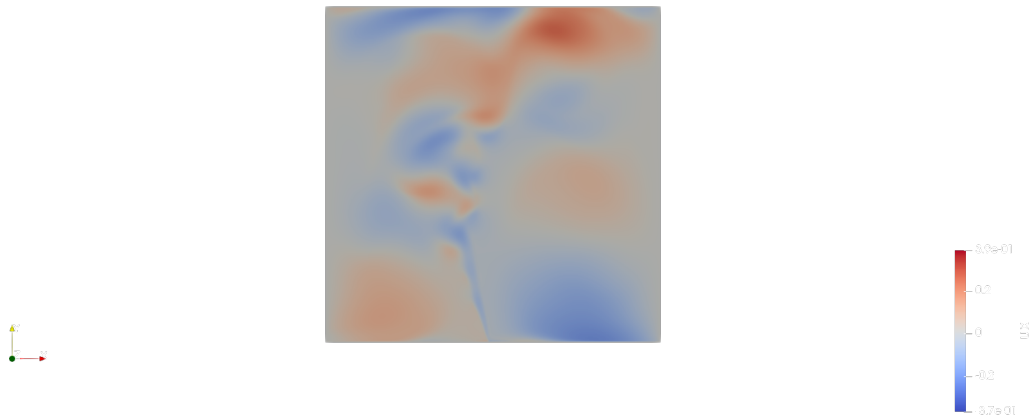

(c) U_x at $t = 100\,\mathrm{s}$

Figure 5: x-component of velocity (U_x) for heater length 0.5 m.

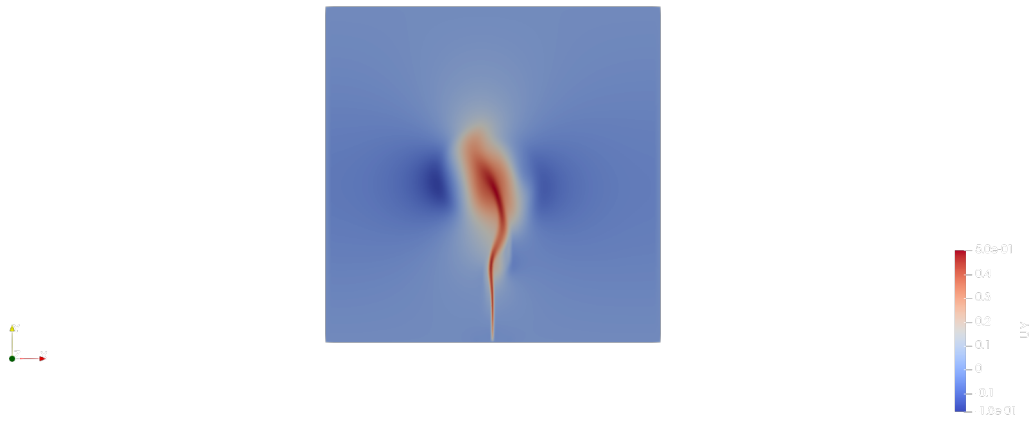

(a) U_y at $t = 25\,\mathrm{s}$

(b) U_y at $t = 50\,\mathrm{s}$

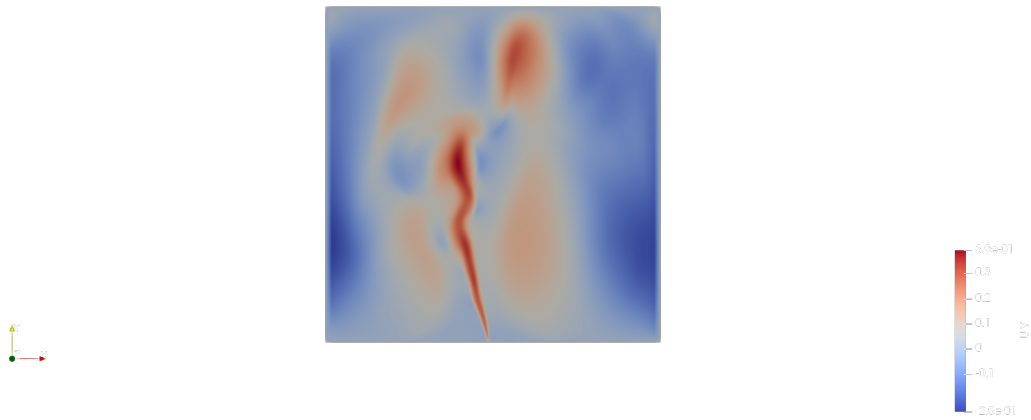

(c) U_y at $t = 100\,\mathrm{s}$

Figure 6: y-component of velocity (U_y) for heater length 0.5 m.

(a) Temperature at $t = 25\,\mathrm{s}$

(b) Temperature at $t = 50\,\mathrm{s}$

(c) Temperature at $t = 100\,\mathrm{s}$

Figure 7: Temperature distribution for heater length 1 m.

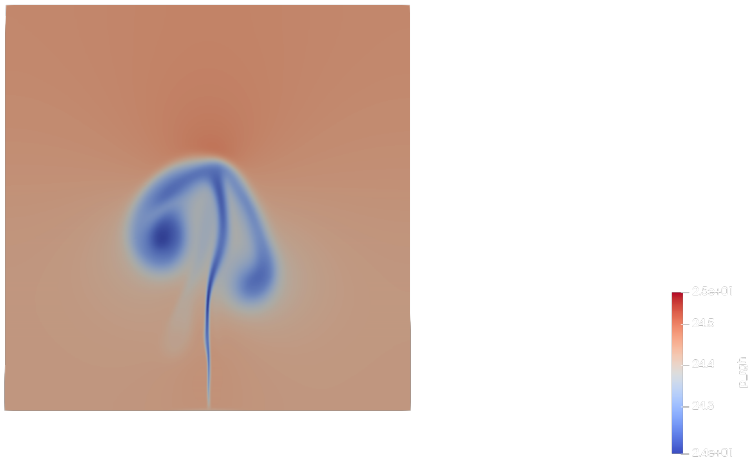

(a) Pressure (p_{rgh}) at $t = 25\,\mathrm{s}$

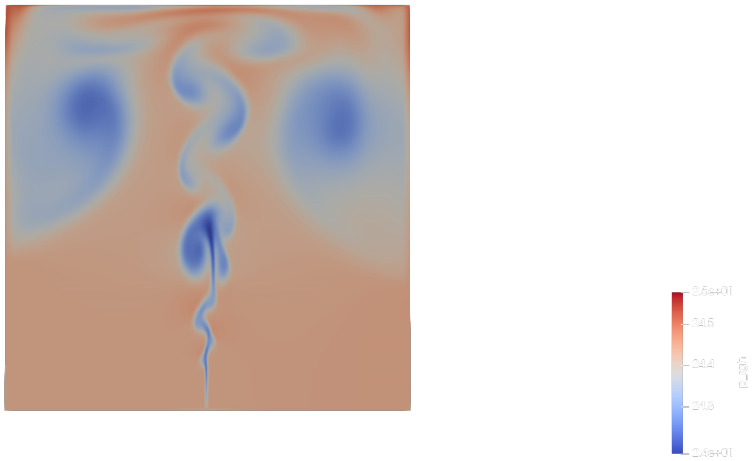

(b) Pressure (p_{rgh}) at $t = 50\,\mathrm{s}$

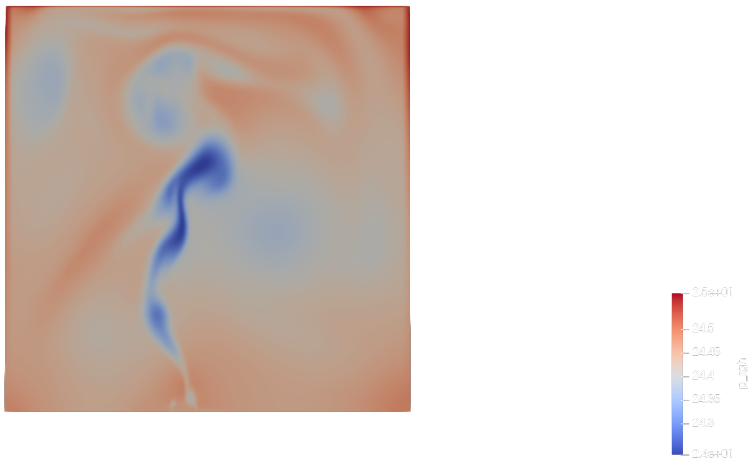

(c) Pressure (p_{rgh}) at $t = 100\,\mathrm{s}$

Figure 8: Pressure distribution for heater length 1 m.

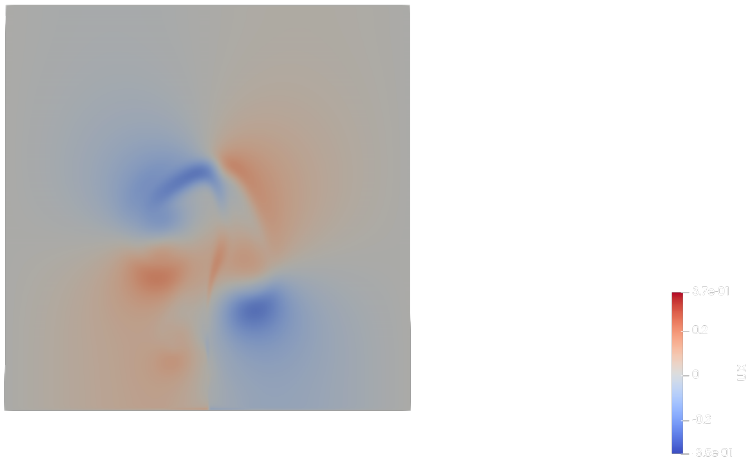

(a) U_x at $t = 25\,\mathrm{s}$

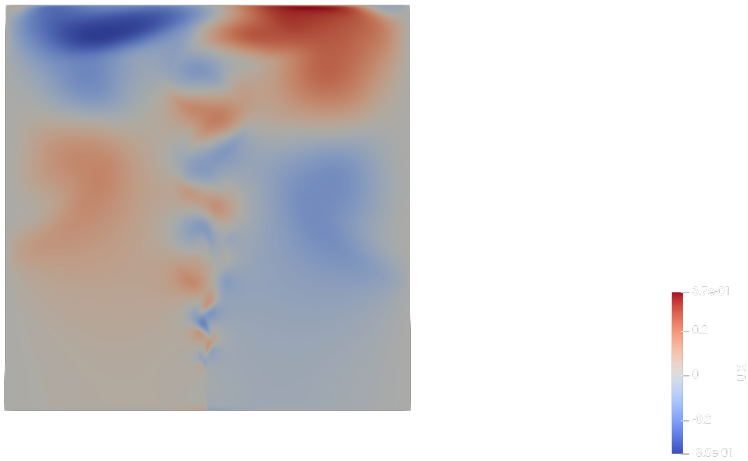

(b) U_x at $t = 50\,\mathrm{s}$

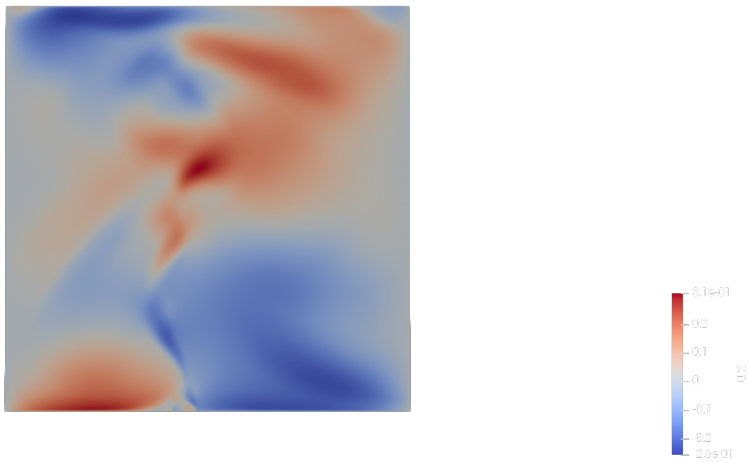

(c) U_x at $t = 100\,\mathrm{s}$

Figure 9: x-component of velocity (U_x) for heater length 1 m.

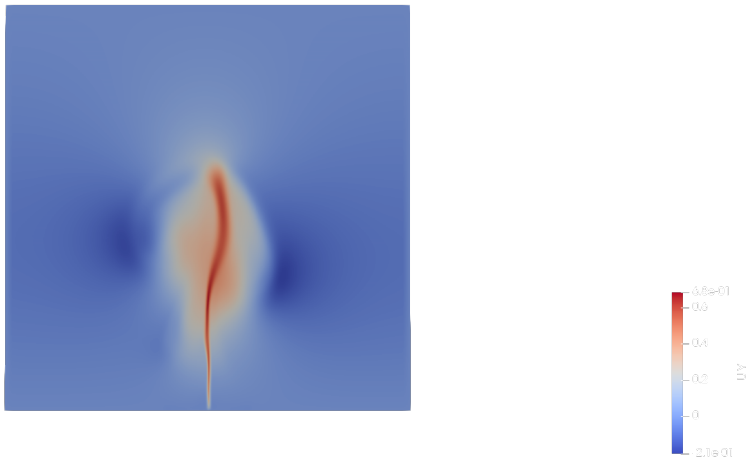

(a) U_y at $t = 25\,\mathrm{s}$

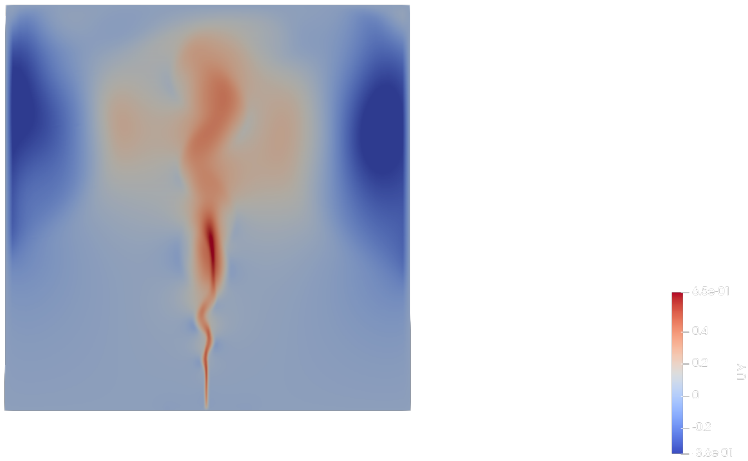

(b) U_y at $t = 50\,\mathrm{s}$

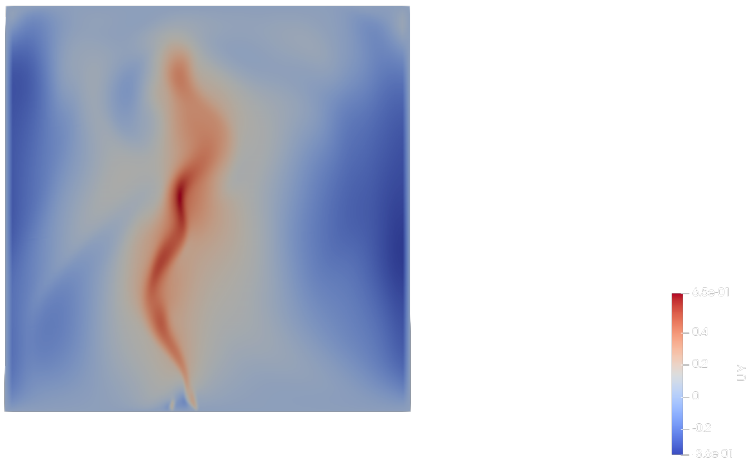

(c) U_y at $t = 100\,\mathrm{s}$

Figure 10: y-component of velocity (U_y) for heater length 1 m.

(a) Temperature at $t = 25\,\mathrm{s}$

(b) Temperature at $t = 50\,\mathrm{s}$

(c) Temperature at $t = 100\,\mathrm{s}$

Figure 11: Temperature distribution for heater length 1.5 m.

(a) Pressure (p_{rgh}) at $t = 25\,\mathrm{s}$

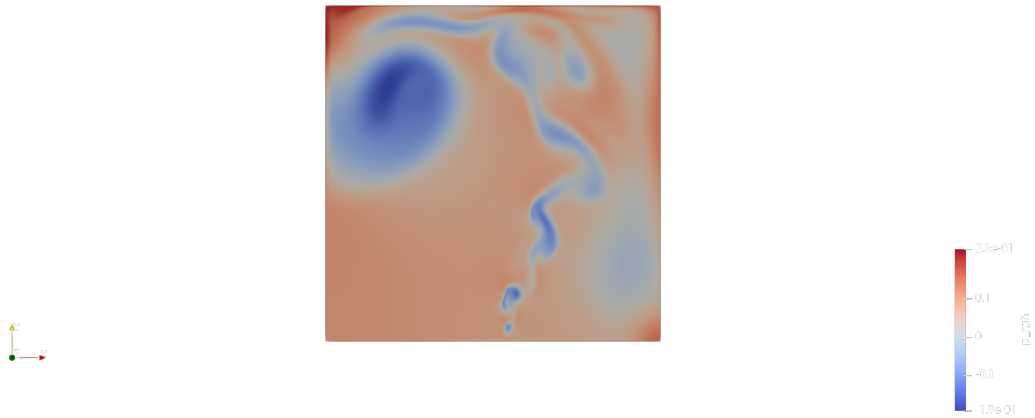

(b) Pressure (p_{rgh}) at $t = 50\,\mathrm{s}$

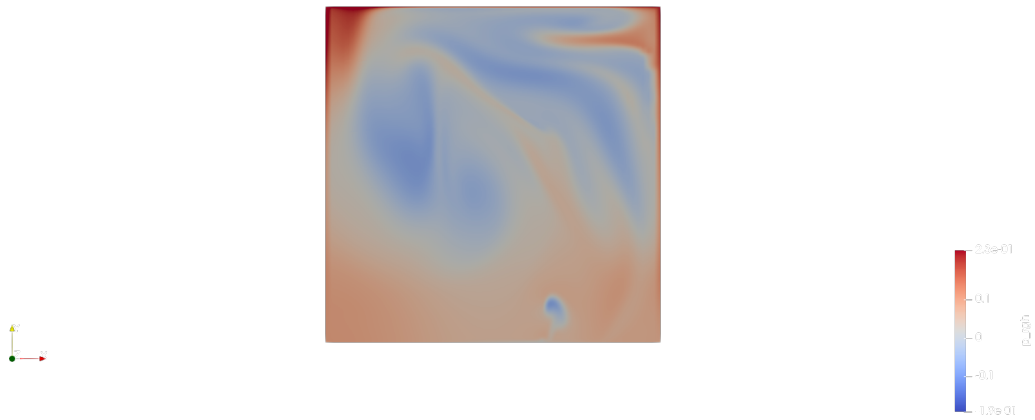

(c) Pressure (p_{rgh}) at $t = 100\,\mathrm{s}$

Figure 12: Pressure distribution for heater length 1.5 m.

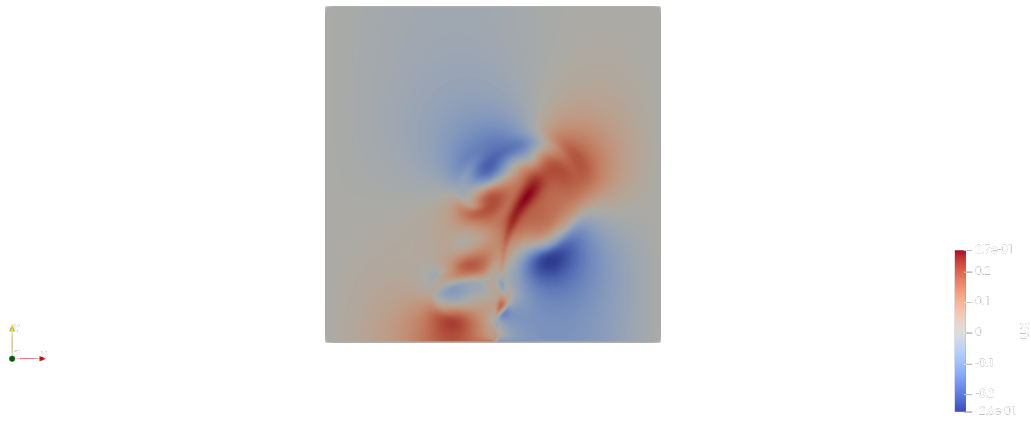

(a) U_x at $t = 25\,\mathrm{s}$

(b) U_x at $t = 50\,\mathrm{s}$

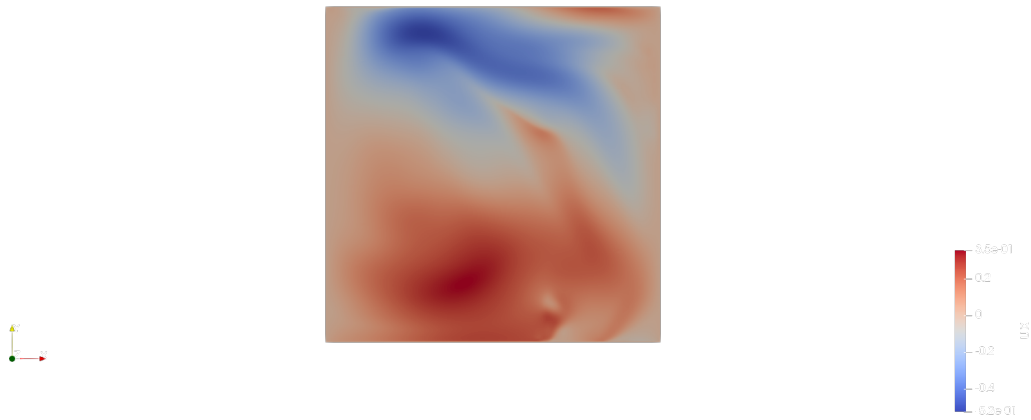

(c) U_x at $t = 100\,\mathrm{s}$

Figure 13: x-component of velocity (U_x) for heater length 1.5 m.

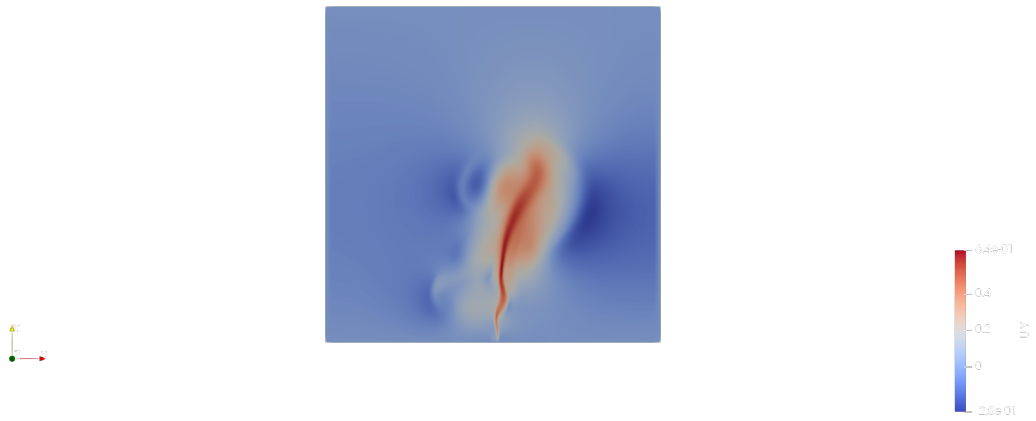

(a) U_y at $t = 25\,\mathrm{s}$

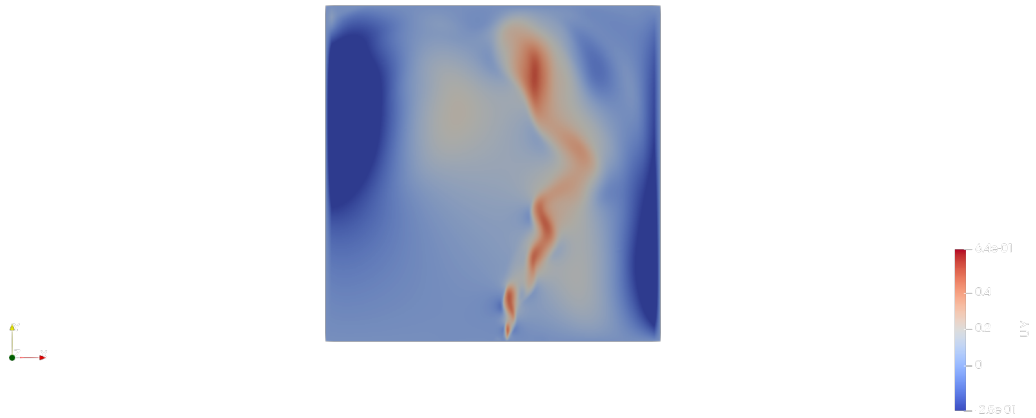

(b) U_y at $t = 50\,\mathrm{s}$

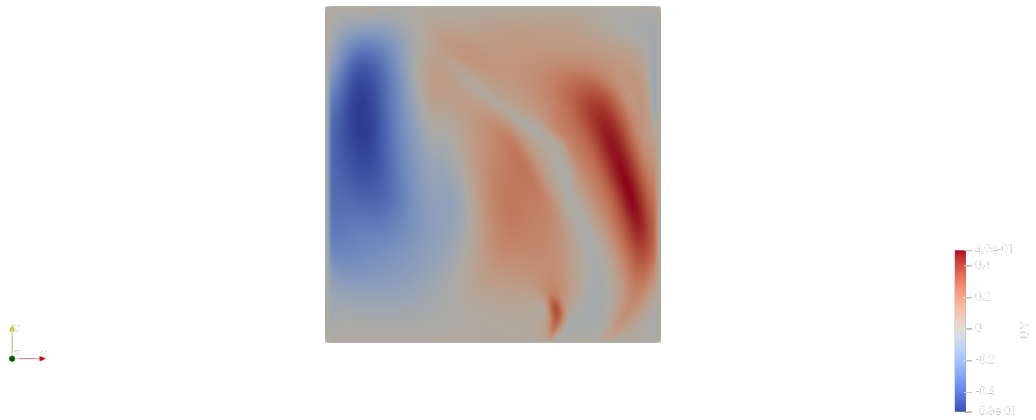

(c) U_y at $t = 100\,\mathrm{s}$

Figure 14: y-component of velocity (U_y) for heater length 1.5 m.

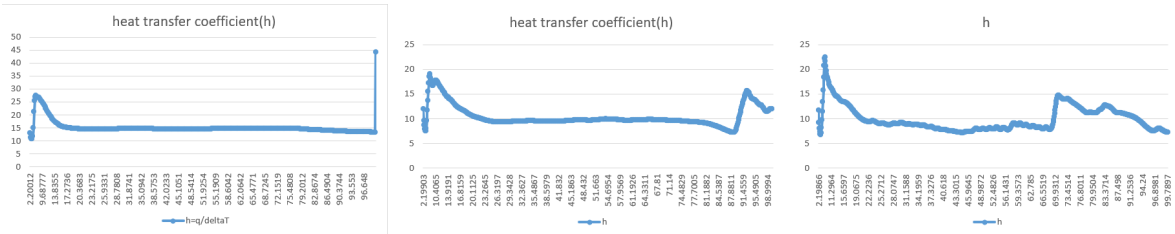

(a) Heater length 0.5 m (b) Heater length 1 m (c) Heater length 1.5 m

Figure 15: Heat transfer coefficient (h) vs. time for different heater lengths.

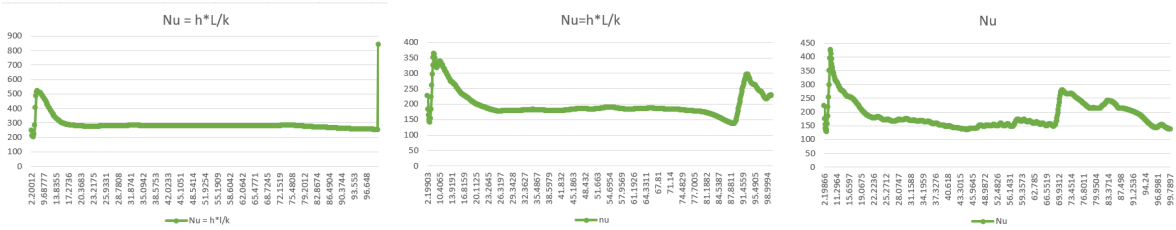

(a) Heater length 0.5 m (b) Heater length 1 m (c) Heater length 1.5 m

Figure 16: Nusselt number (Nu) vs. time for different heater lengths.